Available online at www.sciencedirect.com
ScienceDirect
Ceramics International 37 (2011) 3657–3663
CERAMICS INTERNATIONAL
www.elsevier.com/locate/ceramint

Solvothermal synthesis of microsphere ZnO nanostructures in DEA media

R. Razali [a], A. Khorsand Zak [a,b,*], W.H. Abd. Majid [a], Majid Darroudi [b]

[a] Low Dimensional Material Research Center, Department of physics, Faculty of science, University of Malaya, 50603 Kuala Lumpur, Malaysia
[b] Department of Chemistry, Faculty of Science, Ferdowsi University of Mashhad, 91775-1436 Mashhad, Iran

Received 17 February 2011; received in revised form 13 June 2011; accepted 14 June 2011
Available online 21 June 2011

Abstract

Microsphere ZnO nanostructures (ZnO-MNs) were synthesized via solvothermal method in diethanolamine (DEA) media. DEA was utilized to terminate the growth of ZnO nanoparticles which forms the ZnO-MNs. The ZnO-MNs were characterized by a number of techniques, including X-ray diffraction analysis (XRD) and field emission scanning electron microscopy (SEM). The ZnO-MNs prepared by solvothermal process at the temperature of 150 °C for 6, 12, 18, and 24 h exhibited a hexagonal (wurtzite) structure with sizes ranging from 2 to 4 μm. The growth mechanism and morphology of the ZnO-MNs were also investigated, and it was found that the ZnO-MNs were formed by ZnO nanoparticles with average particle size of 25 ± 5 nm. To show role of DEA in the formation of Zn-MNs, effect of MEA (monoethanolamine) and TEA (triethanolamine) on morphology of the final product are also investigated. The results showed that DEA is a good polymerization agent that can be used as a stabilizer in the solvothermal technique for preparing fine ZnO powder.

Keywords: D. ZnO; Microstructure; Solvothermal; Powder technology

1. Introduction

Zinc oxide (ZnO) is an inorganic semiconductor with a hexagonal wurtzite crystal structure. ZnO has a wide and direct band gap which is nearly 3.37 eV at room temperature, and is transparent in visible light. It is also a reliable luminescence material at both ambient and high temperature as it has a large excision binding energy which is approximately 60 mV [1]. ZnO is also applicable for use in electronic and optoelectronic devices [2], gas sensors [3], solar cells [4], display windows [5], and optical transparency in the visible range [6]. In addition, ZnO is also used in sensors and actuators due to its piezoelectric [7] (especially for high frequency) and pyro-electric properties [8]. This material shows interesting properties in its low dimensional structure. In the nano size range, ZnO is expected to possess interesting physical properties, and profound coupling effect compare to the respective bulk counterpart [9]. Therefore, several new routes have been developed to synthesize ZnO nanostructures such as a wet polymerization method [10], sol–gel [11], sol–gel combustion [12,13], precipitation [14], hydrothermal [15], solvothermal [16], CVD [17], microwave assisted [18], a sonochemical method [19], and thermal oxidation [20]. Recently, investigations have been done to produce ZnO with a hollow structure for special applications such as gas sensing. Tao et al., reported on the preparation of ZnO hollow microspheres with a size distribution from ∼250 nm to ∼4 μm by solvothermal method [21]. Another method by Yu Tian et al., described hollow spheres grown by thermal evaporation [22].

In the present work, microsphere ZnO nanostructures (ZnO-MNs) formed by gathering ZnO nanoparticles were prepared by solvothermal method using zinc acetate solution. Diethanolamine (DEA) was used as a polymerization agent and stabilizer to control the morphology of the product formed by nanostructures. The reaction mechanism has also been investigated. According to the previous studies, the morphology and properties of the product can be changed by kind of solvents, polymerization agents, and solvothermal conditions [23–25]. Therefore, the ZnO nanostructures were prepared in TEA and MEA medias to better explain of the DEA effect on morphology of the final product.

* Corresponding author. Tel.: +60 12 2850849; fax: +60 37 9674146.
E-mail address: alikhorsandzak@gmail.com (A.K. Zak).

0272-8842/$36.00
doi:10.1016/j.ceramint.2011.06.026

2. Experimental

Zinc acetate (Zn $(CH_3COO)_2$ $2H_2O$), ethanol, and diethanolamine (DEA) were used as starting materials. 0.5 M zinc acetate solution was prepared by dissolving 7.68 g of zinc acetate in 35 ml of ethanol. DEA was added to the solution and then the solution was stirred at 60 °C. The molar ratio of DEA/Zn^{2+} was fixed at 1:1. The solution was stirred again at 60 °C for 1 h. After the stirring period, a clear and homogenous solution was obtained. The Zn^{2+} solution was then aged at room temperature for another hour. The solutions were poured in a stainless steel autoclave in a 50 ml Teflon vessel, and placed in the furnace for 6 h at 150 °C. After the expected time the sample was cooled down to room temperature. The formed white precipitates were dispersed in ethanol solution (30% in deionized water). The precipitates were separated by centrifugation of the mixture (4000 rpm for 4 min) and dispersed again in ethanol solution. These washing steps were repeated three times to remove the DEA polymers. Subsequently, the white precipitates were dried in an oven at 60 °C overnight. Another three of the same solutions were prepared and underwent the same solvothermal process for 12, 18, and 24 h, respectively. The next steps were carried out as previously described.

The same experimental procedure was repeated to prepare ZnO nanostructure in MEA and TEA medias by solvothermal method at 150 °C for 18 h.

The prepared microsphere ZnO nanostructures were characterized by powder X-ray diffraction (XRD, Philips, X'pert, Cu K_α), field emission scanning electron microscopy (FESEM), Fourier transform infrared spectroscopy (FTIR-ST-IR\ST-SIR spectrometer). The TEM observations were carried out on a Hitachi H-7100 electron microscope.

3. Results and discussion

3.1. ZnO-MNs formation mechanism

In the solvothermal process, alcohol plays a very important role in contributing the unoccupied oxygen to Zn^{+2} in order to form ZnO [26]. The formed ZnO nanoparticles are attracted to DEA chains because of the ionic-dipolar interaction between the hydrogens atoms in the polymer and oxygen in the ZnO. After that, the DEA chains are attracted together by hydrogen-bonding forces and the small seed of ZnO-MN will be formed. The ZnO-MN will grow since the polymers are associated with each other. The complete process is shown in Fig. 1. As shown

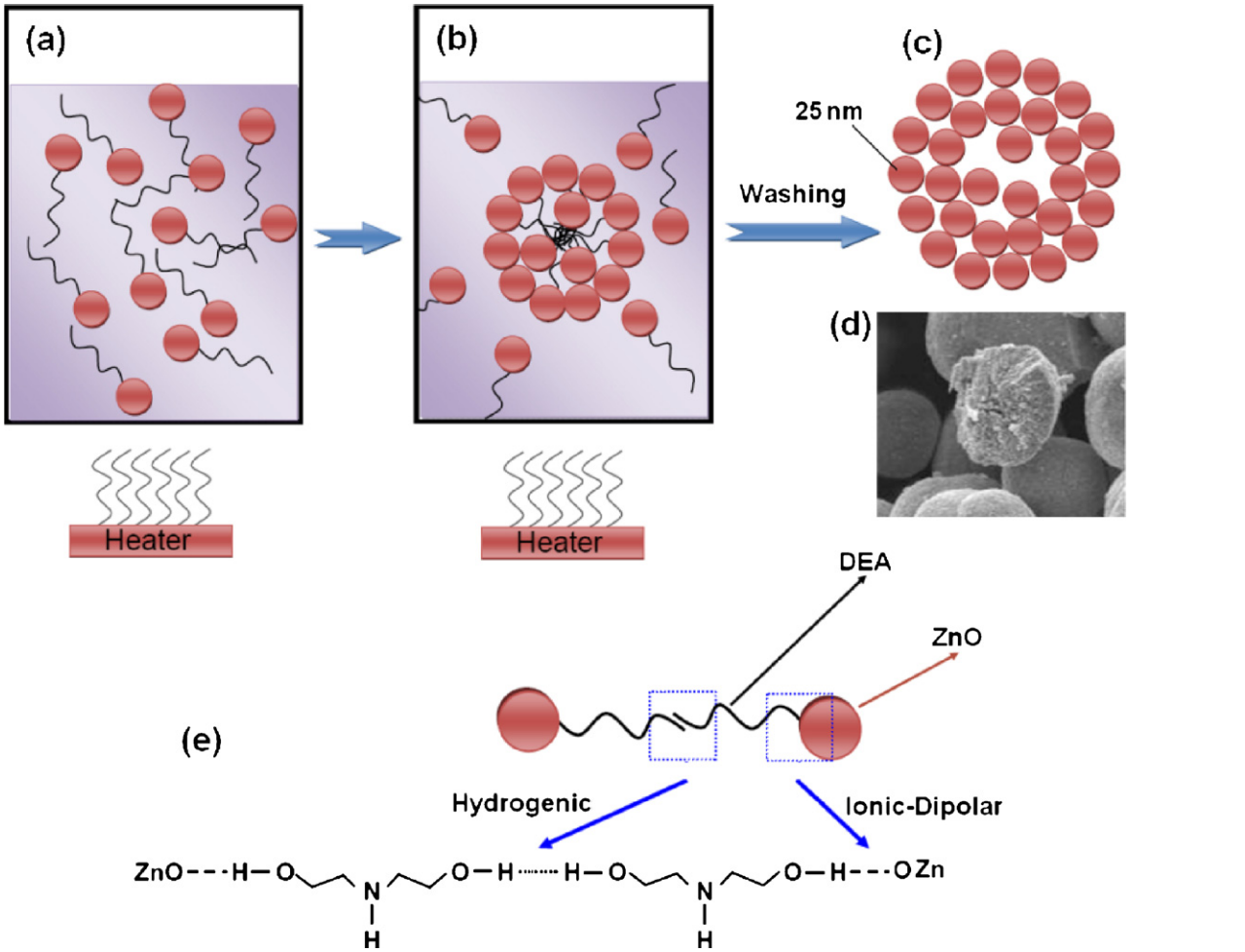

Fig. 1. The formation process of ZnO-MNs. (a) formation of ZnO nanoparticles, (a) formation of ZnO-MNs, (c) ZnO-MNs after washing, (d) cross section image of a ZnO-MN, (e) the bonding formation.

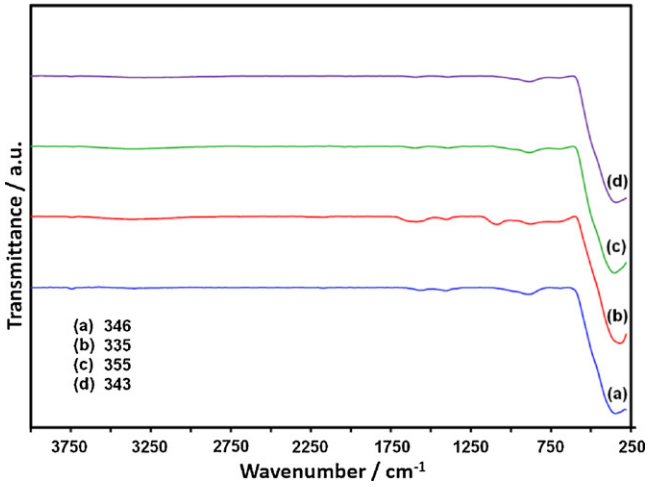

Fig. 2. FTIR pattern of ZnO-MNs prepared at 150 °C for (a) 6 h, (b) 12 h, (c) 18 h, and (d) 24 h.

in Fig. 1d, the density of the ZnO nanoparticles in the core of ZnO-MNs is lesser compared to their surface.

3.2. FTIR analysis

Fig. 2 shows the FTIR spectra of the ZnO samples treated at temperatures of 150 °C and different times. For the FTIR spectra of the prepared samples at 6, 12, 18 and 24 h, no important absorption peaks from 500 to 4000 cm^{-1} can be found, which corresponds to the carboxylate and hydroxyl impurities in the materials. More specifically, the negligible broad band at 3420 cm^{-1} was assigned to the O–H stretching mode of the hydroxyl group.

For all of the samples in this study, a broad absorption band was observed at 346, 335, 355, and 343 cm^{-1} for samples prepared at 6, 12, 18, and 24 h, respectively. These absorption bands correspond to the E_2 mode of hexagonal ZnO (Raman active) [27,28]. There was also an absorption band at around 1150 cm^{-1}. This absorption band can be related to C–O and therefore can be neglected.

3.3. X-ray diffraction (XRD)

The XRD patterns of the ZnO-MNs prepared by solvothermal process at 150 °C for 6, 12, 18, and 24 h are shown in Fig. 3(a–d),

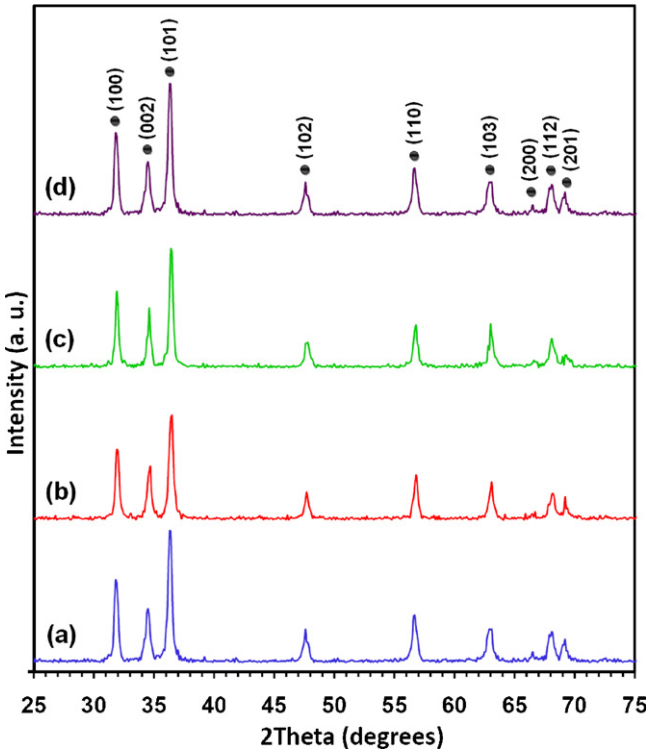

Fig. 3. XRD pattern of ZnO-MNs prepared at 150 °C for (a) 6 h, (b) 12 h, (c) 18 h, and (d) 24 h.

respectively. All detectable peaks can be indexed to ZnO wurtzite structure (PDF card no: 00-036-1451). The wurtzite lattice parameters, for e.g. the values of d – the distances between adjacent crystal planes (hkl), were calculated from the Bragg equation, $\lambda = 2d \sin\theta$. The lattice constants a, b and c; the inter-planar angles, the angle φ between the planes $(h_1k_1l_1)$ of spacing d_1 and the plane $(h_2k_2l_2)$ of spacing d_2; and V, the primary cell volumes, were calculated from the *Lattice Geometry* equation [29]. The (1 0 0) and (0 0 2) planes were used to calculate the lattice parameters of the ZnO-MNs, prepared at 150 °C for 6, 12, 18, and 24 h. The results were summarized in Table 1.

The crystallite sizes of the ZnO-MNs were determined by the means of X-ray line-broadening method using the Scherrer equation: $D = (k\lambda/\beta_{hkl}\cos\theta)$, where D is the crystallite size in nanometers (nm), λ is the wavelength of the radiation (1.54056 Å for CuK_α radiation), k is a constant equal to 0.94, β_{hkl} is the peak width at half-maximum intensity, and θ is

Table 1
The structural parameters of ZnO-MNs prepared at 150 °C for (a) 6, (b) 12, (c) 18, and (d) 24 h.

Heating time (h)	2θ ±0.01	hkl	d_{hkl} (nm) ±0.0005	Structure	Lattice parameter (nm) ±0.005 ±0.01	V (nm^3) ±0.2	cos φ ±0.002
6	31.85	(1 0 0)	0.2807	Hexagonal	$a = 0.324$	47.27	0
	34.50	(0 0 2)	0.2598		$c/a = 1.60$		
12	31.95	(1 0 0)	0.2799	Hexagonal	$a = 0.323$	47.84	0
	34.61	(0 0 2)	0.2589		$c/a = 1.60$		
18	31.91	(1 0 0)	0.2802	Hexagonal	$a = 0.323$	47.02	0
	34.56	(0 0 2)	0.2594		$c/a = 1.61$		
24	31.93	(1 0 0)	0.2800	Hexagonal	$a = 0.323$	47.90	0
	34.60	(0 0 2)	0.2590		$c/a = 1.60$		

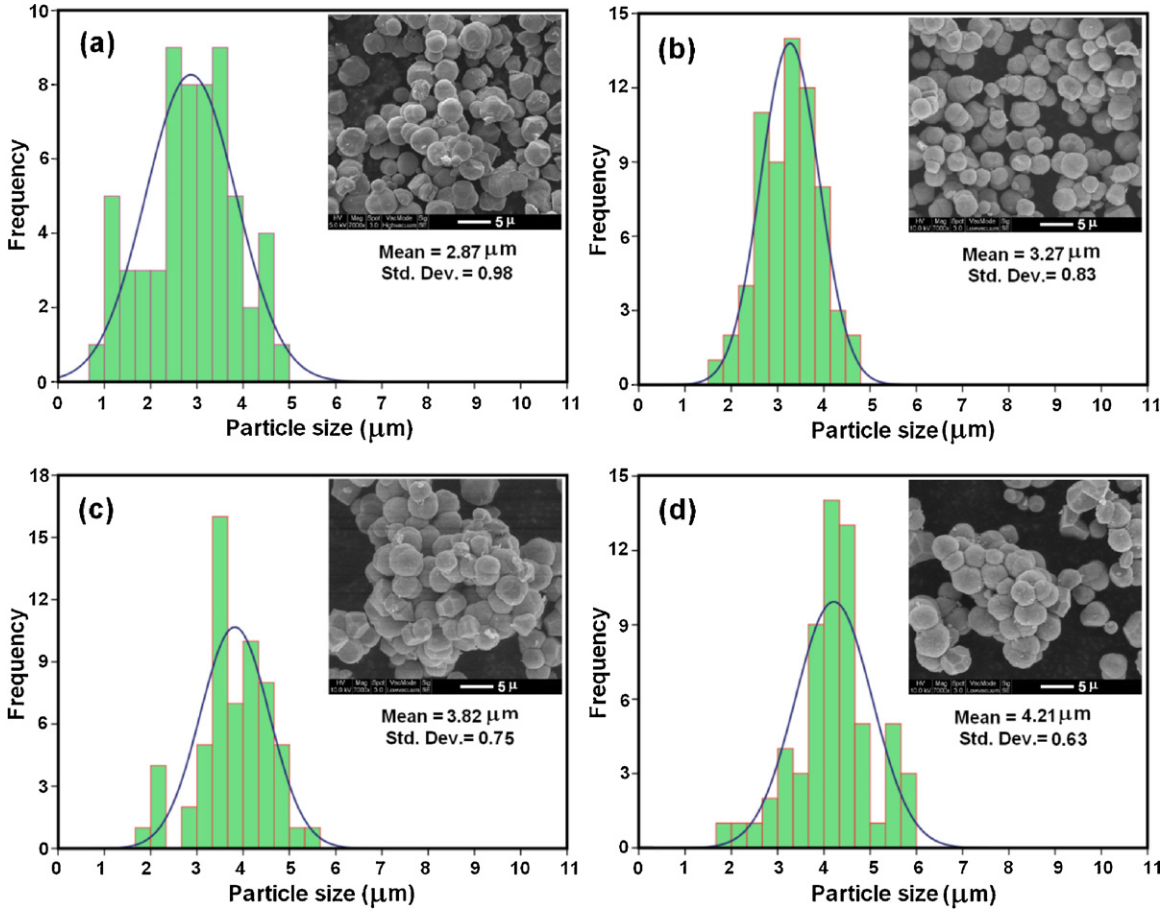

Fig. 4. SEM images of ZnO-MNs prepared at 150 °C for (a) 6 h, (b) 12 h, (c) 18 h, and (d) 24 h.

the peak position. The (1 0 2) plane was chosen to calculate the crystallite size (either plane can be used for this purpose). The crystallite sizes of the ZnO-MNs prepared at 150 °C for 6, 12, 18, and 24 h were observed to be 22 ± 2, 23 ± 2, 24 ± 2, and 23 ± 2 nm, respectively. The crystallite sizes are almost similar and it shows that the size growth of the ZnO nanoparticles will be stopped after 6 h and after this time, the growth of the ZnO-MNs will be continued with agglomeration of the ZnO nanoparticles at the heating duration.

3.4. Morphology study of the ZnO-MNs

The size distribution histograms and SEM of the ZnO-MNs prepared by solvothermal process at 150 °C for 6, 12, 18, and 24 h are shown in Fig. 4(a–d), respectively. It can be observed that the ZnO-MNs grew as the thermal process time increased. It was also observed that the ZnO-MNs prepared at 150 °C for 6, 12, 18, and 24 h appears in spherical shape. The size histograms of the ZnO-MNs show that the main particle size of the ZnO-MNs prepared at temperature of 150 °C for 6, 12, 18, and 24 h were about 2.87 ± 1, 3.27 ± 1, and 3.82 ± 0.75 and 4.21 ± 0.63 μm, respectively.

The detail morphology of the ZnO-MNs prepared at temperature of 150 °C for 12 h was precisely studied in Fig. 5(a–d). Fig. 5a shows that the ZnO-MNs are equal in size and spherical in shape as shown in Fig. 5b at higher magnification. Focusing on a single ZnO-MN (Fig. 5c and d), it is clearly observed that the ZnO-MN was formed with

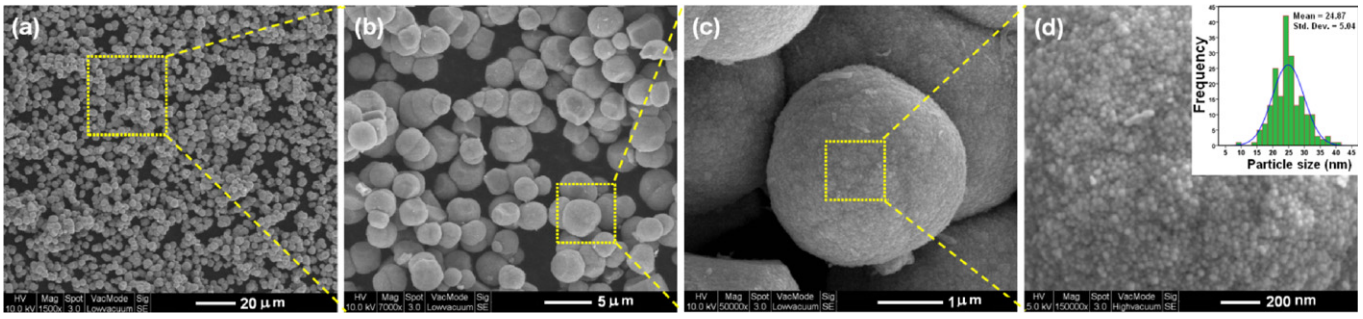

Fig. 5. SEM images of ZnO-MNs prepared at 150 °C for 18 h, in different magnification of (a) 5000, (b) 7000, (c) 50,000, and (d) 150,000.

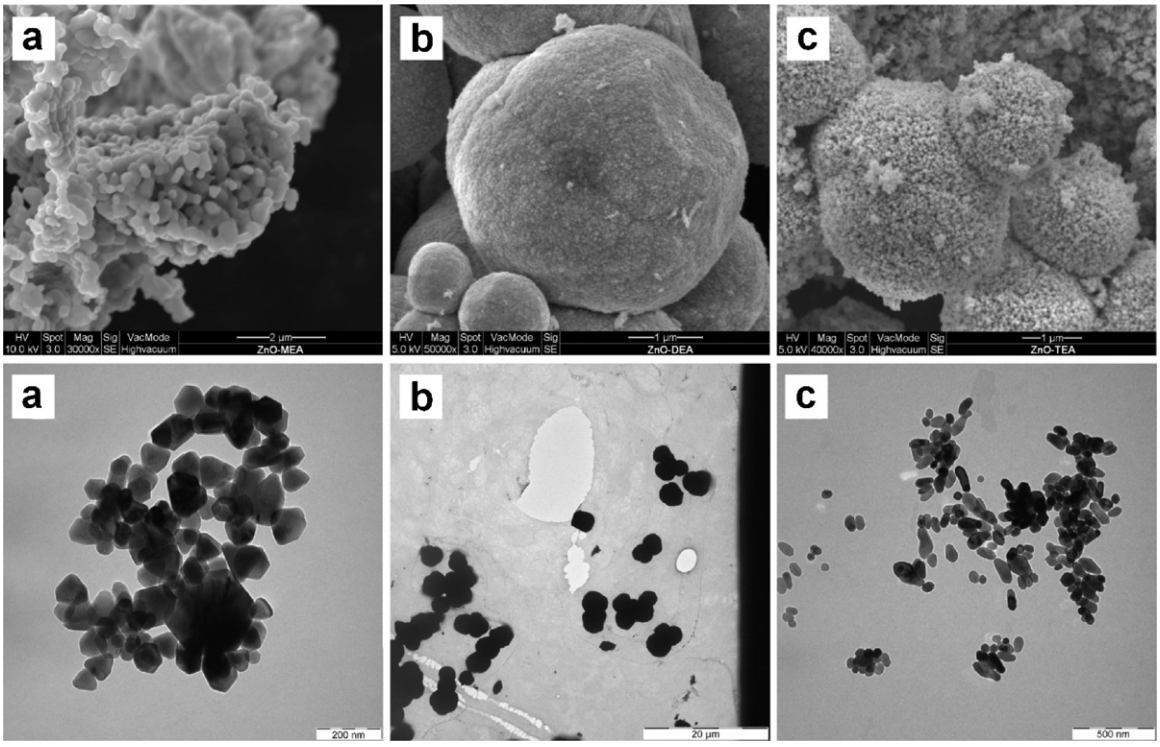

Fig. 6. The SEM and TEM images of ZnO nanostructures prepared in (a) MEA media, (b) DEA media, and (c) TEA media at 150 °C for 18 h.

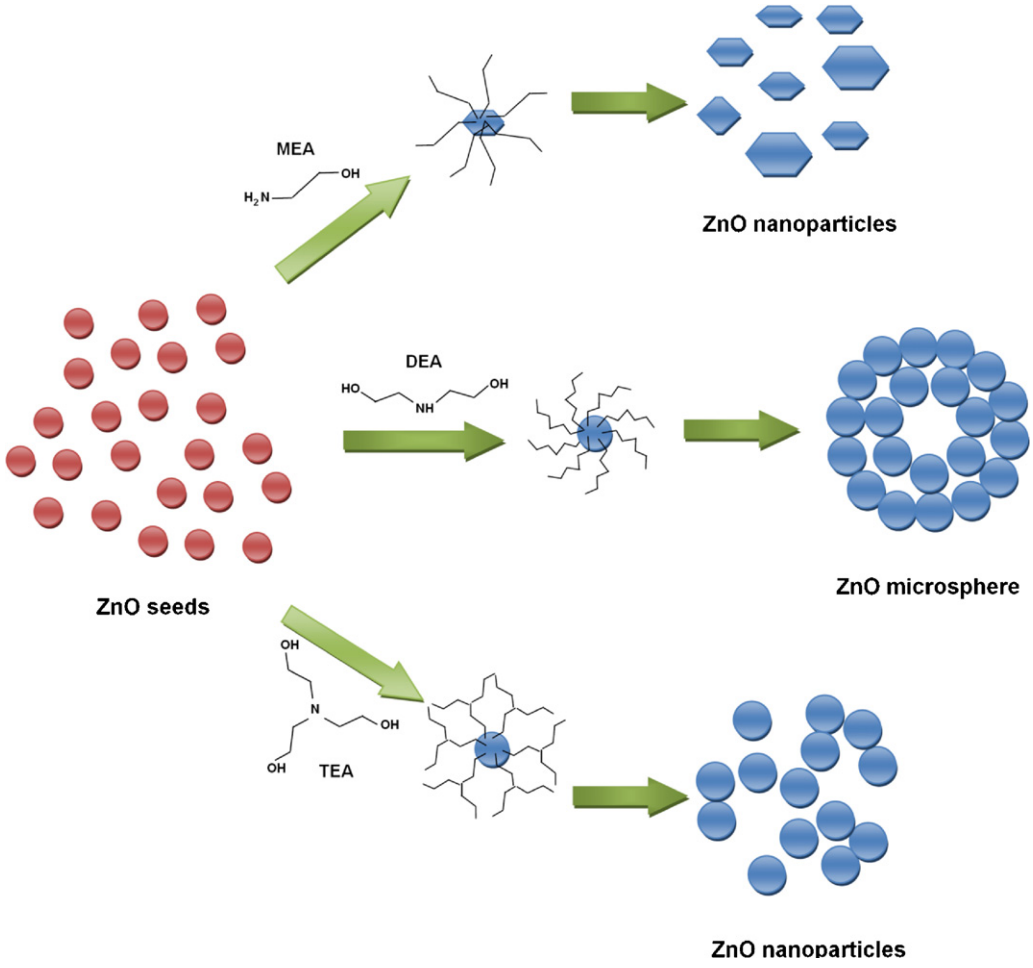

Fig. 7. The effect of ethanolamine family on morphology of ZnO nanostructures.

ZnO nanoparticles, as described earlier. The particle size distribution of the ZnO nanoparticles in the inset of the Fig. 5d shows an average size of 25 ± 5 nm. This result is in good agreement with the XRD measurements as described earlier in the paper.

3.5. Effect of ethanolamine family on morphology of the final product

Fig. 6(a–c) shows the SEM and TEM micrograph of the ZnO nanostructures prepared by solvothermal method at 150 °C for 18 h using MEA, DEA, and TEA, respectively. The powders were dispersed in acetone by ultrasonic bath and then prepared for TEM. From Fig. 6a, both of the TEM and SEM images show freestanding ZnO nanoparticles for the sample that was prepared in MEA media. The SEM image in Fig. 6c shows that the ZnO nanoparticles are sticking together but become easily separated after sonication, as shown in the TEM image of Fig. 6c. But the particles which were prepared in DEA media have retained their microsphere morphology, even after sonication as shown in the SEM and TEM images of Fig. 6b.

The formations of the ZnO-MNs were explained in Section 3.1. Regarding this section, DEA chains acted as a bridge to form the ZnO-MNs and stopped the growth of the ZnO nanoparticles. This can even occur for the sample that was prepared in TEA media. The formed ZnO seeds are attracted to some of the TEA chains, due to the ionic-dipolar interaction between the hydrogen atoms in the polymer and the oxygen in the ZnO. The ZnO-NPs will grow with the association of the ZnO seeds.

On the other hand, some of the TEA chains are attracted to each other by hydrogen-bonding forces. However, TEA has one O-H branch more than DEA. So, porous ZnO-MNs were formed by ZnO nanoparticles, because the polymer chains do not permit the ZnO nanoparticles to reach each other. That is why the nanoparticles are separated easily by sonication. In MEA media, the ZnO seeds became attached to the MEA from the OH end, but there is no bonding between the other ends of the MEA chains. Like before, The ZnO-NPs grow with the association of the ZnO seeds. When the number of reached ZnO seeds increases, the other seeds cannot reach the nanoparticles. Therefore, the growth of nanoparticles will be eliminated. See Fig. 7.

4. Conclusion

ZnO-MNs were synthesized by solvothermal method in DEA media. From the XRD results, it was observed that all the ZnO-MNs prepared by solvothermal process at temperature of 150 °C for 6, 12, 18, and 24 h exhibited the hexagonal, wurtzite structure and the FTIR results show that the high purity of the samples. The average diameter of the ZnO-MNs prepared at temperature of 150 °C for 6, 12, 18, and 24 h were 2.87 ± 1, 3.27 ± 1, and 3.82 ± 0.75 and 4.21 ± 0.63 μm, respectively. The ZnO-MNs were formed by ZnO nanoparticles with an average particle size of 25 ± 5 nm. The morphology studies of samples prepared in MEA and TEA media confirm that the DEA is a good polymer agent and plays an important role to prepare ZnO-MNs.

Acknowledgements

This work was supported by the University of Malaya through grants no: UM.C/625/1/HIR/041. Authors are gratefully acknowledgment Dr. Reza Mahmoudian for his supporting.

References

[1] Z.L. Wang, ZnO nanowire and nanobelt platform for nanotechnology, Mater. Sci. Eng. R: Rep. 64 (2009) 33–71.
[2] C.E. Kim, P. Moon, I. Yun, S. Kim, J.M. Myoung, H.W. Jang, J. Bang, Process estimation and optimized recipes of ZnO:Ga thin film characteristics for transparent electrode applications, Expert Syst. Appl. 38 (2011) 2823–2827.
[3] S.J. Kim, P.S. Cho, J.H. Lee, C.Y. Kang, J.S. Kim, S.J. Yoon, Preparation of multi-compositional gas sensing films by combinatorial solution deposition, Ceram. Int. 34 (2008) 827–831.
[4] L. Lu, R. Li, K. Fan, T. Peng, Effects of annealing conditions on the photoelectrochemical properties of dye-sensitized solar cells made with ZnO nanoparticles, Sol Energy 84 (2010) 844–853.
[5] D. Kim, Influence of CuSn thickness on the work function and optoelectrical properties of ZnO/CuSn/ZnO multilayer films, Displays 31 (2010) 155–159.
[6] Y. Natsume, H. Sakatau, Zinc oxide films prepared by sol–gel spin-coating, Thin Solid Films 372 (2000) 30–36.
[7] M.K. Gupta, N. Sinha, B.K. Singh, N. Singh, K. Kumar, B. Kuma, Piezoelectric, dielectric, optical and electrical characterization of solution grown flower-like ZnO nanocrystal, Mater. Lett. 63 (2009) 1910–1913.
[8] C.S. Wei, Y.Y. Lin, Y.C. Hu, C.W. Wu, C.K. Shih, C.T. Huang, S.H. Chan, Partial-electroded ZnO pyroelectric sensors for responsivity improvement, Sens. Actuators A 128 (2006) 18–24.
[9] M. Law, J. Goldberger, P. Yang, Semiconductor nanowires and nanotubes, Annu. Rev. Mater. Res. 34 (2004) 83–122.
[10] K.L. Ying, T.E. Hsieh, Y.F. Hsieh, Colloidal dispersion of nano-scale ZnO powders using amphibious and anionic polyelectrolytes, Ceram. Int. 35 (2009) 1165–1171.
[11] A.K. Zak, W.H. Abd Majid, M. Darroudi, R. Yousefi, Synthesis and characterization of ZnO nanoparticles prepared in gelatin media, Mater. Lett. 65 (2011) 70–73.
[12] Vânia C. de Sousa, Márcio R. Morelli, Ruth H.G. Kiminami, Combustion process in the synthesis of ZnO–Bi_2O_3, Ceram. Int. 26 (2000) 561–564.
[13] A.K. Zak, M.E. Abrishami, W.H. Abd Majid, R. Yousefi, S.M. Hosseini, Effects of annealing temperature on some structural and optical properties of ZnO nanoparticles prepared by a modified sol–gel combustion method, Ceram. Int. 37 (2011) 393–398.
[14] Y. Wang, C. Zhang, S. Bi, G. Luo, Preparation of ZnO nanoparticles using the direct precipitation method in a membrane dispersion micro-structured reactor, Powder Technol. 202 (2010) 130–136.
[15] C.H. Lu, C.H. Yeh, Influence of hydrothermal conditions on the morphology and particle size of zinc oxide powder, Ceram. Int. 26 (2000) 351–357.
[16] J. Ma, C. Jiang, Y. Xiong, G. Xu, Solvent-induced growth of ZnO microcrystals, Powder Technol. 167 (2006) 49–53.
[17] R. Yousefi, M.R. Muhamad, A.K. Zak, Investigation of indium oxide as a self-catalyst in ZnO/ZnInO heterostructure nanowires growth, Thin Solid Films 518 (2010) 5971–5977.
[18] Y. Cao, B. Liu, R. Huang, Z. Xia, S. Ge, Flash synthesis of flower-like ZnO nanostructures by microwave-induced combustion process, Mater. Lett. 65 (2011) 160–163.
[19] P. Mishra, R.S. Yadav, A.C. Pandey, Growth mechanism and photoluminescence property of flower-like ZnO nanostructures synthesized by starch-assisted sonochemical method, Ultrason. Sonochem. 17 (2010) 560–565.

[20] C.H. Xu, H.F. Lui, C. Surya, Synthetics of ZnO nanostructures by thermal oxidation in water vapor containing environments, Mater. Lett. 65 (2011) 27–30.
[21] J. Tao, Controllable preparation of ZnO hollow microspheres by self-assembled block copolymer Original Research Article, Colloids Surf. A: Physicochem. Eng. Aspects 330 (2008) 67–71.
[22] Y. Tian, H.B. Lu, L. Liao, J.C. Li, Y. Wu, Q. Fu, Controlled growth surface morphology of ZnO hollow microspheres by growth temperature Original Research Article, Physica E 41 (2009) 729–733.
[23] S.K.N. Ayudhya, P. Tonto, O. Mekasuwandumrong, V. Pavarajarn, P. Praserthdam, Solvothermal synthesis of ZnO with various aspect ratios using organic solvents, Cryst. Growth Des. 6 (2006) 2446–2450.
[24] L. Xu, Y.L. Hu, C. Pelligra, C.H. Chen, L. Jin, H. Huang, S. Sithambaram, M. Aindow, R. Joesten, S.L. Suib, ZnO with different morphologies synthesized by solvothermal methods for enhanced photocatalytic activity, Chem. Mater. 21 (2009) 2875–2885.
[25] M. Distaso, R.N.K. Taylor, N. Taccardi, P. Wasserscheid, W. Peukert, Influence of the counterion on the synthesis of ZnO mesocrystals under solvothermal conditions, Chem. Eur. J. 17 (2011) 2923–2930.
[26] M. Niederberger, N. Pinna, Metal Oxide Nanoparticles in Organic Solvents: Synthesis, Formation, Assembly and Application, Springer-Verlag, London, 2009.
[27] G. Xiong, U. Pal, J.G. Serrano, K.B. Ucer, R.T. Williams, Photoluminesence and FTIR study of ZnO nanoparticles: the impurity and defect perspective, Phys. Stat. Sol. C 10 (2006) 3577–3581.
[28] A. Kaschner, U. Haboeck, M. Strassburg, Ma Strassburg, G. Kaczmarczyk, A. Hoffmann, C. Thomsen, A. Zeuner, H.R. Alves, D.M. Hofmann, B.K. Meyer, Nitrogen-related local vibrational modes in ZnO:N, Appl. Phys. Lett. 80 (2002) 1909–1911.
[29] A.K. Zak, W.H. Abd Majid, M.E. Abrishami, R. Yousefi, Solid State Sci. 13 (2011) 251–256.